Available online at www.sciencedirect.com
SCIENCE DIRECT®
Journal of Power Sources 123 (2003) 190–199
JOURNAL OF POWER SOURCES
www.elsevier.com/locate/jpowsour

A semi-empirical model of the direct methanol fuel cell performance Part I. Model development and verification

P. Argyropoulos, K. Scott*, A.K. Shukla, C. Jackson

Chemical and Process Engineering Department, University of Newcastle Upon Tyne, Merz Court, Newcastle Upon Tyne NE1 7RU, UK

Received 2 September 2002; received in revised form 1 April 2003; accepted 14 April 2003

Abstract

A model equation is developed to predict the cell voltage versus current density response of a liquid feed direct methanol fuel cell (DMFC). The equation is based on a semi-empirical approach in which methanol oxidation and oxygen reduction kinetics are combined with effective mass transport coefficients for the fuel cell electrodes. The model equation is validated against experimental data for a small-scale fuel cell and is applicable over a wide range of methanol concentration and temperatures.

Keywords: Direct methanol fuel cell; Model; Performance

1. Introduction

Characterisation of fuel cells frequently uses large and complex computer models, based on minute details of cell component design (physical dimensions, materials, etc.) along with chemical and physical considerations (transport phenomena, electrochemical kinetics, etc.). The codes, often proprietary, needed in the design and development of fuel cells, are cumbersome and time-consuming for use in system analysis models. Simpler approaches are normally used for system studies. Another approach, which is not time and cost efficient, would be to conduct appropriate tests at every condition expected to be analysed in the system. Alternatively, it is prudent to develop correlations, based on thermodynamic modelling, that describe cell performance as operating conditions, such as temperature and pressure are changed [1]. Thermodynamic modelling is used to depict the equations so that only a limited number of tests are needed to define design constants within the equation.

In the development of model equations to predict performance of polymer electrolyte fuel cells a number of approaches using empirical models have been attempted [2–7]. In many cases an excellent agreement between the model and experimental data is achieved by adjusting appropriate coefficients/parameters in the model equations. However, a major limitation is that the coefficients do not follow any specific trends with fuel cell operating variables and do not allow any physically real interpretation of the model. Such an approach has also been applied to the case of the direct methanol fuel cell (DMFC) [8].

Direct methanol fuel cells have reached a significant stage of development with high power density performance now achieved. Probably without exception the research and development of the DMFC to reach high performance targets has proceeded with anodes of the binary alloy of Pt and Ru. In general, the performance of the DMFC depends on the MEA construction method, the materials and the operating conditions in the cell. It is well documented that increasing cell temperature above approximately 60 °C causes a significant increase in power performance and that at 90 °C and beyond power densities above 200 mW cm^{-2}, are achievable. This level of power performance is typically achieved using a pressurised cathode oxygen or air (2–5 bar). The use of oxygen gives the best performance but most terrestrial applications require the use of air. In addition, many potential applications of the DMFC will require air under almost ambient conditions of temperature and pressure.

In this paper, we develop a semi-empirical model for the cell voltage, current density response of the DMFC which is based on Tafel type kinetics for methanol oxidation and oxygen reduction and on measured mass transport coefficients. The model equation is validated against experimental data obtained for a small-scale fuel cell.

* Corresponding author. Tel.: +44-191-222-8771; fax: +44-191-222-5292.
E-mail address: k.scott@ncl.ac.uk (K. Scott).

0378-7753/$ – see front matter © 2003 Elsevier B.V. All rights reserved.
doi:10.1016/S0378-7753(03)00558-5

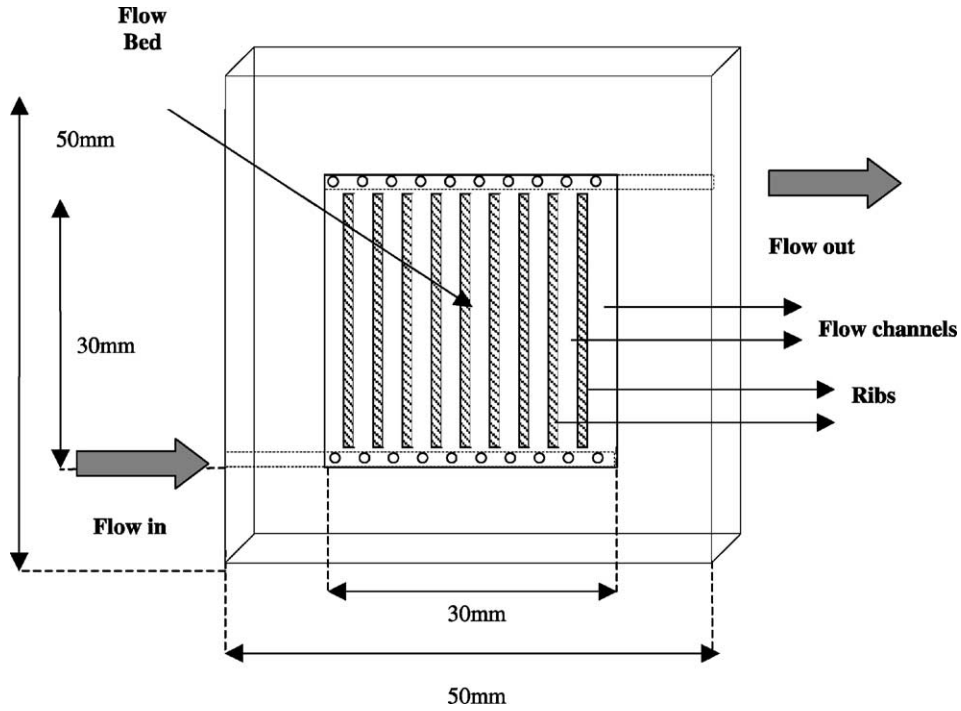

Fig. 1. DMFC small-scale cell flow bed design and manifold arrangement.

2. Experimental

Tests on the DMFC were performed with a cell with a cross-sectional area of 9 cm^2. The cell consisted of two non-porous graphite blocks with a series of parallel channels machined into the block for the flow of methanol and oxygen/air (Fig. 1).

The cell was fitted with a membrane electrode assembly (MEA) sandwiched between the two graphite blocks. The cell was held together between two plastic insulation sheets and two stainless steel backing plates using a set of retaining bolts positioned around the periphery of the cell. Electrical heaters, supplied by Watson Marlow, were placed behind each of the graphite blocks to heat the cell to the desired operating temperature. The graphite blocks were also provided with electrical contacts and small holes to accommodate thermocouples. The fuel cells were used in a simple flow rig, which consisted of a Watson Marlow peristaltic pump to supply aqueous methanol solution, from a reservoir, to a Eurotherm temperature controller to maintain the cell at a constant temperature. Air was supplied from cylinders, at ambient temperature, and the pressure regulated by needle valves.

MEAs studied in this work were made in the following manner: the anode consisted of a Teflonised (20%) carbon cloth support (E-Tek, type 'A'), of 0.3 mm thickness, upon which was spread a thin (diffusion layer) layer of uncatalysed (ketjenblack 600) 10 wt.% teflonised carbon. The catalysed layer, unless otherwise specified consisted of 35 wt.% Pt–15 wt.% Ru (2 mg cm^{-2} metal loading) dispersed on carbon (ketjen) and bound with bound with 10 wt.% Nafion® from a solution of 5 wt.% Nafion® dissolved in a mixture of water and lower aliphatic alcohol's (Aldrich), was spread on this diffusion backing layer. A thin layer of Nafion® solution was spread onto the surface of each electrode. Electrode preparation are described in detail elsewhere [10]. The cathode was constructed using a similar method as for the anode, using a thin diffusion layer bound with 10 wt.% PTFE, and 1 mg cm^{-2} Pt black with 10 wt.% Nafion® in the catalyst layer. The electrodes were placed on opposite sides of a pre-treated Nafion® 117 membrane. This pre-treatment involved boiling the membrane for 1 h in 5 vol.% H_2O_2 and 1 h in 1 mol dm^{-3} H_2SO_4 before washing in boiling Millipore water (>18 mΩ) for 2 h with regular changes of water. The assembly was hot-pressed at 100 kg cm^{-2} for 3 min at 135 °C.

Cell voltage versus current density response was measured galvanostatically, by incrementally increasing the current from open circuit and measuring the cell potential and then reducing the current incrementally again measuring the cell voltage. The data reported here were obtained with one MEA, unless otherwise stated. The MEA was conditioned before use in two stages: for 48 h in the test cell, in 2.0 mol dm^{-3} methanol solution at 75 °C, and then by maintaining the cell with an applied load of 100 mA cm^{-2} for several hours. This pre-treatment resulted in stable performance under continuous operation. Data used in this empirical modelling has been presented earlier in a previous publication [11].

3. Overall cell voltage

It is well known that useful work (electrical energy) is obtained from a fuel cell only when a reasonable current is drawn, and that the actual cell potential falls below its equilibrium potential because of several irreversible losses: catalyst polarisation, internal resistance and mass transport.

In general, the overall cell voltage E_{cell} has several components:

(i) Equilibrium potentials, determined from the Nernst equation, of cathode and anode reactions (E_{e}^{C} and E_{e}^{A}), which make up the reversible cell voltage, E_{e}.
(ii) Overpotentials at the cathode and the anode, η_{a} and η_{c}.
(iii) Ohmic losses in the electrolytes ($IR_{\text{electrolyte}}$), the cell separator (IR_{sep}), the electrodes and in the connections from the power supply to the electrodes ($IR_{\text{circ}}^{\text{C}} IR_{\text{circ}}^{\text{A}}$).

From the above, the cell voltage can be presented in the form:

$$E_{\text{cell}} = E_{\text{e}}^{\text{C}} - E_{\text{e}}^{\text{A}} - |\eta_{\text{c}}| - |\eta_{\text{a}}| - IR_{\text{circ}}^{\text{C}} - IR_{\text{circ}}^{\text{A}} - IR_{\text{electrolyte}} - IR_{\text{separator}} \quad (1)$$

The overpotentials at electrodes arise from various polarisation phenomena and increase in magnitude as the rate of reaction, or the current density, increases. The electrode design and material should also facilitate efficient gas release from its surface to ensure that the *IR* drop in the electrolyte and the "bubble polarisation" is low. The material of the current connectors should be highly conducting and designed to the thickness required to carry anticipated maximum cell currents. The electrode material should also, if possible be highly conducting and be of the required thickness. A low electrical resistance of the electrodes is also desirable to achieve a uniform potential distribution over the face of the electrode. The practical size of the electrodes is often limited by these two considerations.

3.1. Electrode polarisation

The objective of a fuel cell is to convert as much of the fuel as possible to the product, the maximum amount of the work which may be derived from the fuel will be that corresponding to $-\Delta G$ after conversion, i.e. at the product exit of the fuel cell. There, $-\Delta G$ will be less negative than the value at reactant inlet, since the concentration of the reactant will have fallen and correspondingly that of the product will have risen. Thus, the maximum voltage E_{max} that a fuel cell can develop under reversible conditions at real conversions is given by

$$nFE_{\text{max}} = -\Delta G = -\Delta G_T^0 + RT \ln\left(\frac{C_{\text{r}}}{(C_p)^m}\right) \quad (2)$$

where n is the number of electrons exchanged per molecule of reactant, F the Faraday constant, R the gas constant, $-\Delta G_T^0$ is the Gibbs energy of the reaction under standard concentration (activity) conditions at operating temperature T (K); C_{r} and C_p are the ratios of concentrations (or more exactly activities) of reactant and product leaving the fuel cell to those in the standard state, and m is the reaction order of product relative to that of the reactant.

The polarisation losses are determined by the kinetics of the electrode reactions, by the physical structure (geometry) of the cell and by the type of electrode used. From a practical point of view, the "overvoltage" is the voltage difference, which is measured between the "open circuit voltage" and the "terminal voltage" under the conditions of current flowing in either direction. Tafel's equation is typically used to represent overvoltage, η:

$$\eta = a + b \ln j_{\text{c}} = a + b \ln(nFk) \quad (3)$$

where j_{c} is the cathodic current density (A cm^{-2}), k the rate expressed ($\text{mol cm}^{-2}\,\text{s}^{-1}$), n the number of electrons successively transferred per reacting molecule, and a and b are constants for a given reaction and substrate, at a given temperature. The Tafel constant b is

$$b = -\frac{RT}{\alpha F} \quad (4)$$

where α_{c} is the cathodic transfer coefficient.

The negative sign indicates that the cathodic current density increases as V decreases. In the anodic direction (e.g. hydrogen oxidation), the corresponding equation has constant α' and b', where b' is equal to $RT/\alpha' F$. For cases commonly encountered:

$$\alpha_{\text{c}} = n' + \beta(n_{\text{rds}}) \quad (5)$$

$$\alpha_{\text{a}} = n'' + (1 - \beta)(n_{\text{rds}}) \quad (6)$$

where α_{a} is the corresponding transfer coefficient, β is called the symmetry factor, n' the number of electrons which are transferred in the reaction sequence before each single rate-determining step (rds) in the cathodic direction, in which (n_{rds}) electrons are transferred, and n'' is the number similarly transferred in the anodic direction; (n_{rds}) can only be 1 (for an electrochemical rds) or 0 (for a chemical rds). Thus

$$a_{\text{c}} + a_{\text{a}} = n \quad (7)$$

where n is the number of electrons transferred in the overall process per unit rds.

The net electrode reaction is the sum of the anodic (positive current) and cathodic (negative current) processes and is given by the Butler–Volmer expression:

$$j = j_{\text{o}}[\text{e}^{(a_{\text{a}} F\eta/RT)} - \text{e}^{-(a_{\text{c}} F\eta/RT)}] \quad (8)$$

3.2. Empirical equations for PEMFC

Srinivasan et al. [2] showed that it is possible to use a simple equation to describe the cell voltage versus current

density behaviour for PEMFCs in the activation and Ohmic controlled current density region:

$$E = E_o - b \log j - R_e j \quad (9)$$

$$E_o = E_r + b \log j_o \quad (10)$$

where E_r is the reversible cell potential, b is the Tafel slope for oxygen reduction and R is the Ohmic resistance of the solid polymer electrolyte.

Using Eq. (1) it was shown that as current density is increased the predicted cell potential, with the appropriate coefficients, decreases much less rapidly than observed [3]. To increase the reliability of the aforementioned equation Kim et al. introduced a more complex equation:

$$E = E_o - b \log i - R_e i - m e^{ni} \quad (11)$$

where m and n are parameters that account for the "mass transport overpotential" as a function of current density.

Parameter m affects both the slope of the linear region of the E versus j plot and the current density at which there is a departure from the linearity. The value of n has a predominant effect in the mass transport limitation region. Kim reported that despite the excellent fit when applying Eq. (11) to experimental data they were not able to find a theoretical explanation for the last term of their equation [3]. Lee and Lalk proposed [4–6] a slightly modified form of Kim's equation by adding the ratio of cell pressure to oxygen partial pressure

$$V = E_o - b \log I - R_e I - m \exp^{nI} - b \log \left(\frac{P_{O_2}}{P} \right) \quad (12)$$

More recently Squadrito et al. [7] used Eq. (11) as a starting point and he tried to analyse the different contributions to the mass transport limitation. He considered two different contributions; an Ohmic one which is independent of the current density and a non-Ohmic one which varies with current density and produced an equation in the form:

$$E = E_o - b \log i - R_e i + a i^k \ln(1 - \beta i) \quad (13)$$

where a, k and β are coefficients.

The logarithmic term $\ln(1 - \beta i)$ introduces a limit to the available current density. For $k = 1$, a has the same dimension of R_e and can be interpreted as an additional resistance term due to the overall mass transport limitation. The parameter k mainly influences the point at which there is a departure from linearity and a determines the shape of the curve at high current densities.

Both empirical Eqs. (12) and (13) include several coefficients, which we have used to give good agreement with DMFC fuel cell polarisation data [8]. However, as with the equivalent PEM cell model, changes in the operating conditions, e.g. methanol concentration, produced different values of the empirical coefficients and the predictability of the model, outside a narrow parameter domain, was lost. Thus, it is important to establish models that incorporate the physics and chemistry of the system to enable good prediction of behaviour over a broad range of parameters and variables.

4. An empirical equation for modelling liquid DMFC behaviour

The DMFC is a complex porous electrode system due to the thin three-dimensional structure of the electrocatalyst regions, the porous diffusion layers and the generation of carbon dioxide gas. The DMFC exhibits limiting current behaviour due to mass transport limitations of methanol supply to the anode catalyst caused by the following.

(i) Hydrodynamic mass transfer from the feed flow to the surface of the surface of the carbon cloth backing layer, where the gas bubbles are released into the flowing methanol solution.
(ii) Diffusion mass transfer in the carbon cloth and anode carbon diffusion layer.
(iii) Diffusion mass transfer in the catalyst layer.

Mass transport limiting currents, place a potentially large restriction on the performance of the DMFC and indicates the need for effective electrode design and suitable mass transport analysis. The combined effect of (i) and (ii) is simply expressed as

$$\frac{1}{k_{eff}} = \frac{1}{k_\ell} + \frac{1}{k_{cl}} \quad (14)$$

where the effective mass transfer coefficients, k_{eff}, can be determined at the limiting current from

$$k_{eff} = \frac{j}{nFC_{ME}} \quad (15)$$

where C_{ME} is the methanol concentration.

k_ℓ is the hydrodynamic mass transport coefficient, given by

$$k_l = r(\tfrac{1}{3} j)^p \quad (16)$$

where $p = 0.32$ and $r = 1.87 \times 10^{-6}$ for the fuel cell considered in this paper [11].

The value of k_ℓ depends on the hydrodynamics in the channel as well as on gas bubble liberation at the surface.

k_{cl} is the carbon cloth mass transport coefficient, given by

$$k_{cl} = k_{cl}^o e_c^m \quad (17)$$

where e_c is the liquid voltage, $m = 1.5$, and $k_{cl}^o = (D_{meoh}/\ell_{cl})$, where ℓ_{cl} is the effective backing layer thickness.

In practice, mass transport in the backing layers is unlikely to be governed solely by diffusion as liquid and gas flow in the channels and gas evolution will cause "mixing" in regions facing the flow channel and thus reduce the effective thickness of the carbon backing.

The porous electrocatalyst layer is initially considered as a thin pseudo two-dimensional structure where, due to the potential distribution, highest activity is at a region next to the membrane surface.

The above model Eq. (15) predicts that mass transfer coefficients for the DMFC will exhibit a broad maximum in value with increasing methanol concentration. The model

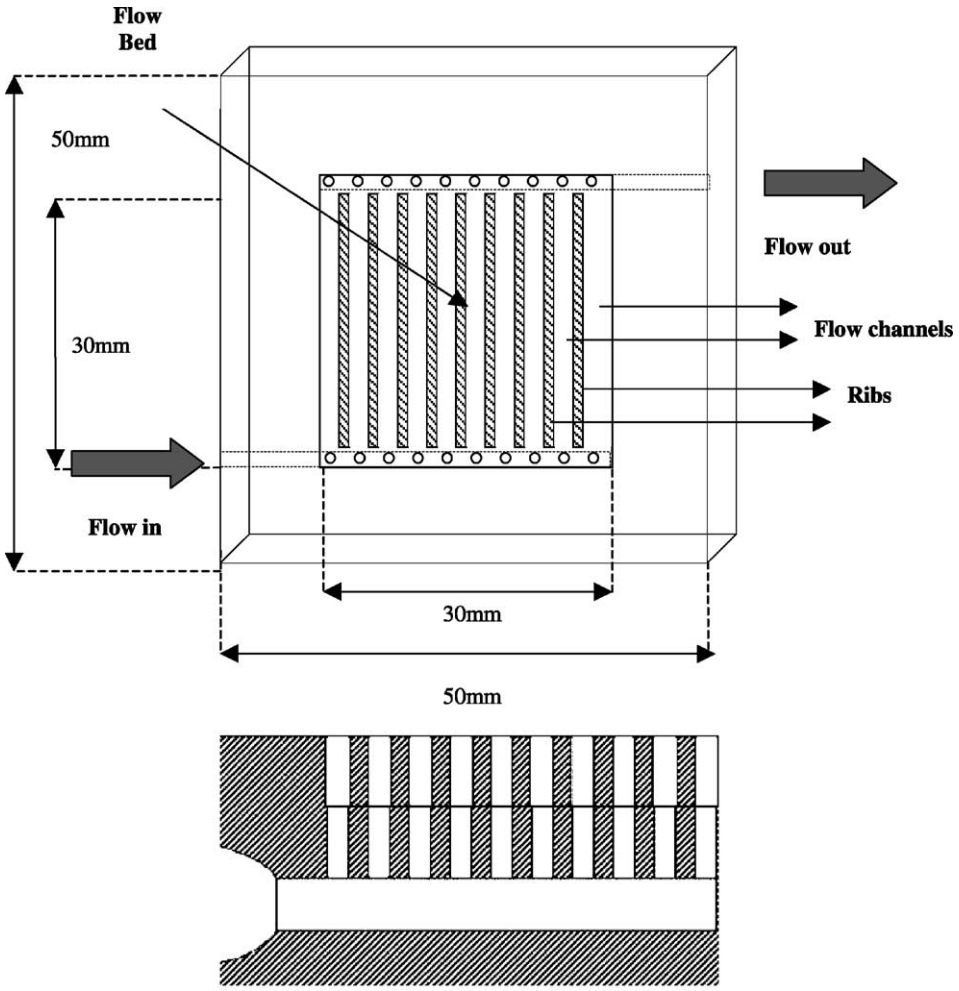

Fig. 2. Effective mass transfer coefficients for the direct methanol fuel cell determined at limiting current conditions. Points are experimental data.

gives reasonable agreement with experimentally measured mass transport coefficients for the DMFC (Fig. 2). The mass transport coefficients are in the range of approximately $(2.5–6.0) \times 10^{-6}\,\mathrm{m\,s^{-1}}$ for a MEA under consideration in this paper.

As a model for methanol oxidation, Tafel type kinetics is chosen:

$$j = j_\mathrm{o} \frac{(C^\mathrm{a}_\mathrm{ME})^N}{C^\mathrm{ref}_\mathrm{ME}} \exp\left[\frac{\alpha F}{RT}(E - E_\mathrm{o})\right] \tag{18}$$

where j_o is the exchange current at the reference concentration, and α the transfer coefficient, a refers to the condition at the anode catalyst surface and N is an order of reaction.

Recent data obtained in this laboratory has confirmed the applicability of the Tafel approximation for methanol oxidation, for a specific electrode assemble considered in this paper [12]. Although we use the Tafel approximation for electrode kinetics we develop an empirical equation for the full range of current densities; from zero to high values. This clearly is an approximation at low current densities (overpotential) but this region of operation is not of real practical interest in fuel cell operation.

We represent mass transport in the anode side of the cell using the effective mass transport coefficient

$$j = k_\mathrm{eff} nF(C_\mathrm{ME} - C^\mathrm{a}_\mathrm{ME}) \tag{19}$$

By re-arranging the previous equation the overpotential becomes

$$(E - E_\mathrm{o})_\mathrm{a} = \frac{RT}{\alpha F}\left[\ln\frac{j}{(C^\mathrm{a}_\mathrm{ME})^N} - \ln\frac{j_\mathrm{o}}{C^\mathrm{ref}_\mathrm{ME}}\right] \tag{20}$$

By combining Eqs. (19) and (20) we obtain

$$(E - E_\mathrm{o})_\mathrm{a} = \frac{RT}{\alpha F}\left[\ln\frac{jC^\mathrm{ref}_\mathrm{ME}}{j_\mathrm{o}C^N_\mathrm{ME}} - N\ln\left(1 - \frac{j}{nFk_\mathrm{eff}C_\mathrm{ME}}\right)\right] \tag{21}$$

Using Eq. (21) for the anode we can obtain an expression for the cell voltage by introducing the kinetic expression for oxygen reduction:

$$j = j_\mathrm{oc}\left[\frac{p_\mathrm{O}}{p^\mathrm{ref}_\mathrm{O}} \exp\left(-\frac{\alpha F\eta_\mathrm{c}}{RT}\right)\right] \tag{22}$$

where p_O is the partial pressure for oxygen.

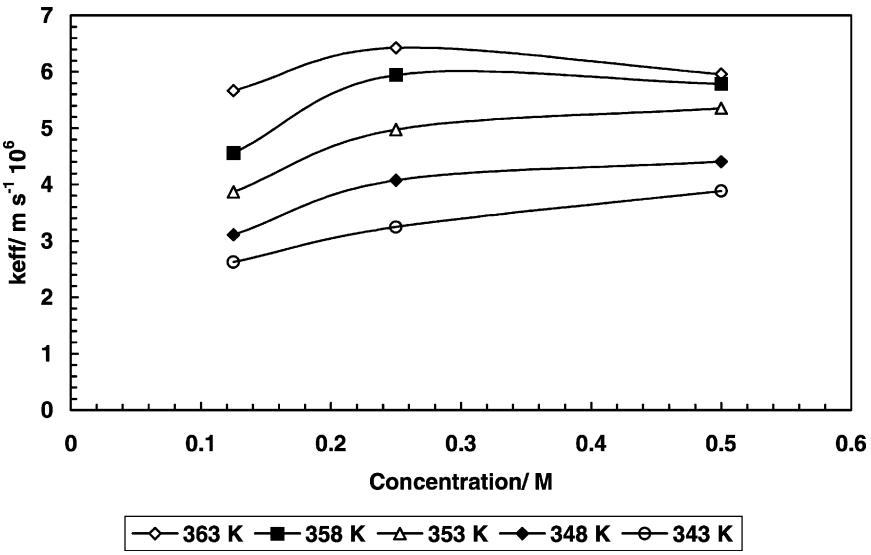

Fig. 3. Comparison between experimental data [11] and empirical equation based prediction for a cell operated with 0.125 M methanol solution supplied at a rate of 1.12 $cm^3\,min^{-1}$ with air fed cathodes pressurised at 2 bar (cell temperatures: (○) 343.15; (◆) 348.15 K; (△) 353.15 K; (■) 358.15 K; (◇) 363.15 K).

The cathode overpotential is then

$$(E - E_o)_c = \frac{RT}{\alpha_c F}\left[\ln\frac{jp_O^{ref}}{j_{oc}p_O} - \ln\left(1 - \frac{j}{nFk_{lO}p_O}\right)\right] \quad (23)$$

where k_{lO} is the mass transport coefficient for the cathode side of the cell.

Combining Eqs. (21) and (23), we obtain an expression for the cell voltage, E_{cell}, as

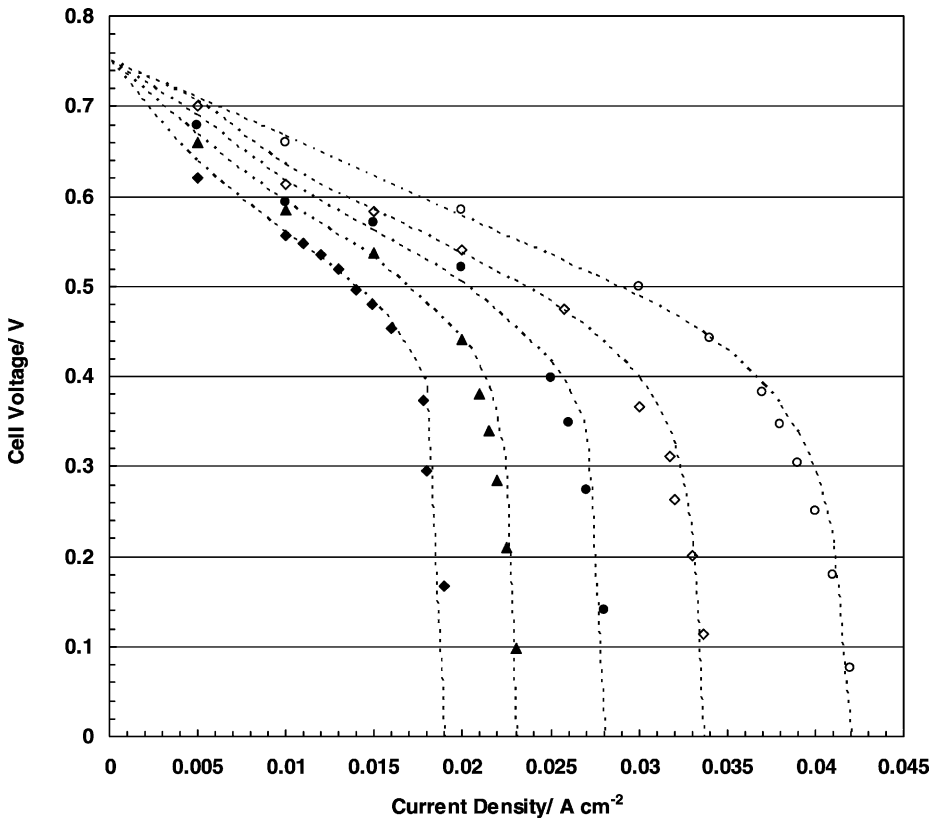

Fig. 4. Comparison between experimental data [11] and empirical equation based prediction for a cell operated with 0.25 M methanol solution supplied at a rate of 1.12 $cm^3\,min^{-1}$ with air fed cathodes pressurised at 2 bar (cell temperatures: (◆) 343.15; (▲) 348.15 K; (●) 353.15 K; (◇) 358.15 K; (○) 363.15 K).

$$E_{\text{cell}} = E_{\text{O cell}} - R_{\text{e}} j - \frac{RT}{F}\left(\frac{1}{\alpha_{\text{a}}} + \frac{1}{\alpha_{\text{c}}}\right) \ln j - \frac{RT}{\alpha_{\text{c}} F}\left[\ln \frac{p_{\text{O}}^{\text{ref}}}{j_{\text{oc}} p_{\text{O}}} - \ln\left(1 - \frac{j}{nFk_{\text{lO}} p_{\text{O}}}\right)\right] - \frac{RT}{\alpha_{\text{a}} F}\left[\ln \frac{C_{\text{ME}}^{\text{ref}}}{j_{\text{o}} C_{\text{ME}}^{N}} - N \ln\left(1 - \frac{j}{nFk_{\text{eff}} C_{\text{ME}}}\right)\right] \quad (24)$$

In many cases, the reduction of oxygen will not proceed under mass transport limitations and we can write Eq. (24) in a simplified form as

$$E_{\text{cell}} = E_{\text{O}}^{*} - b_{\text{cell}} \log j - R_{\text{e}} j + C_1 \ln(1 - C_2 j)$$

where

$$b_{\text{cell}} = \frac{2.303RT}{F}\left(\frac{1}{\alpha_{\text{a}}} + \frac{1}{\alpha_{\text{c}}}\right), \qquad C_1 = \frac{NRT}{\alpha_{\text{a}} F},$$

$$C_2 = \frac{1}{nFk_{\text{eff}} C_{\text{ME}}},$$

$$E_{\text{O}}^{*} = E_{\text{O cell}} - \frac{RT}{\alpha_{\text{c}} F} \ln\left(\frac{p_{\text{O}}^{\text{ref}}}{j_{\text{oc}} p_{\text{O}}}\right) - \frac{RT}{\alpha_{\text{a}} F}\left(\ln \frac{C_{\text{ME}}^{\text{ref}}}{j_{\text{o}} C_{\text{ME}}^{N}}\right) \quad (25)$$

The above equation is a similar form to the Squadrito equation with $k = 0$.

5. Model validation

Eq. (25) above was used to model the cell voltage response of a small-scale single DMFC cell [11]. Model predictions are presented for four different aqueous methanol solution concentrations namely 0.125, 0.25, 0.5 and 0.75 M and for a range of cell operating temperatures. As it can be seen from Figs. 3–6 that the predictions are good. The advantage of the model equation lies in the ability to follow exactly the voltage profile in the limiting current region.

A few comments are necessary regarding the limiting current operating region of the DMFC. As can be seen from the figures there are two types of variation in voltage with current density, depending on the cell operating conditions. One is a steep fall in voltage with current density and is typical of cells operated under severe mass transport limitations or under poor reaction kinetics (low temperatures, low methanol concentrations, or combination of both). The other pattern is a more gradual fall in voltage and is similar to that commonly seen for hydrogen fuel cells.

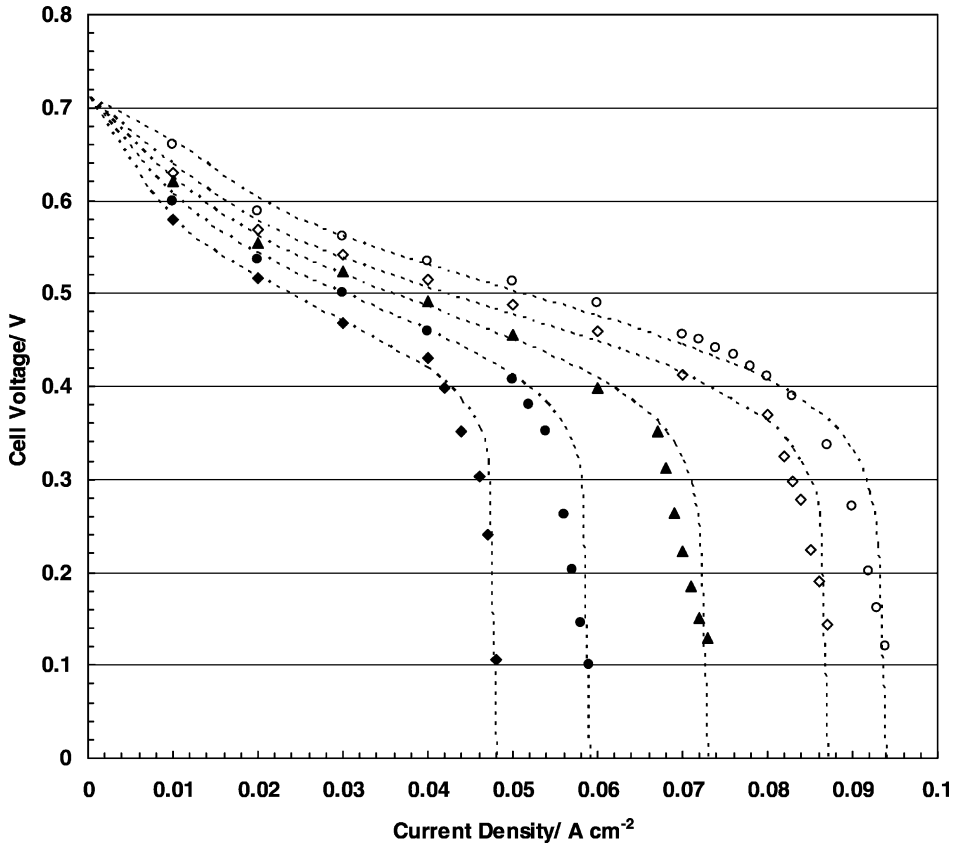

Fig. 5. Comparison between experimental data [11] and empirical equation based prediction for a cell operated with 0.5 M methanol solution supplied at a rate of 1.12 $\text{cm}^3\,\text{min}^{-1}$ with air fed cathodes pressurised at 2 bar (cell temperatures: (◆) 343.15; (●) 348.15 K; (▲) 353.15 K; (◇) 358.15 K; (○) 363.15 K).

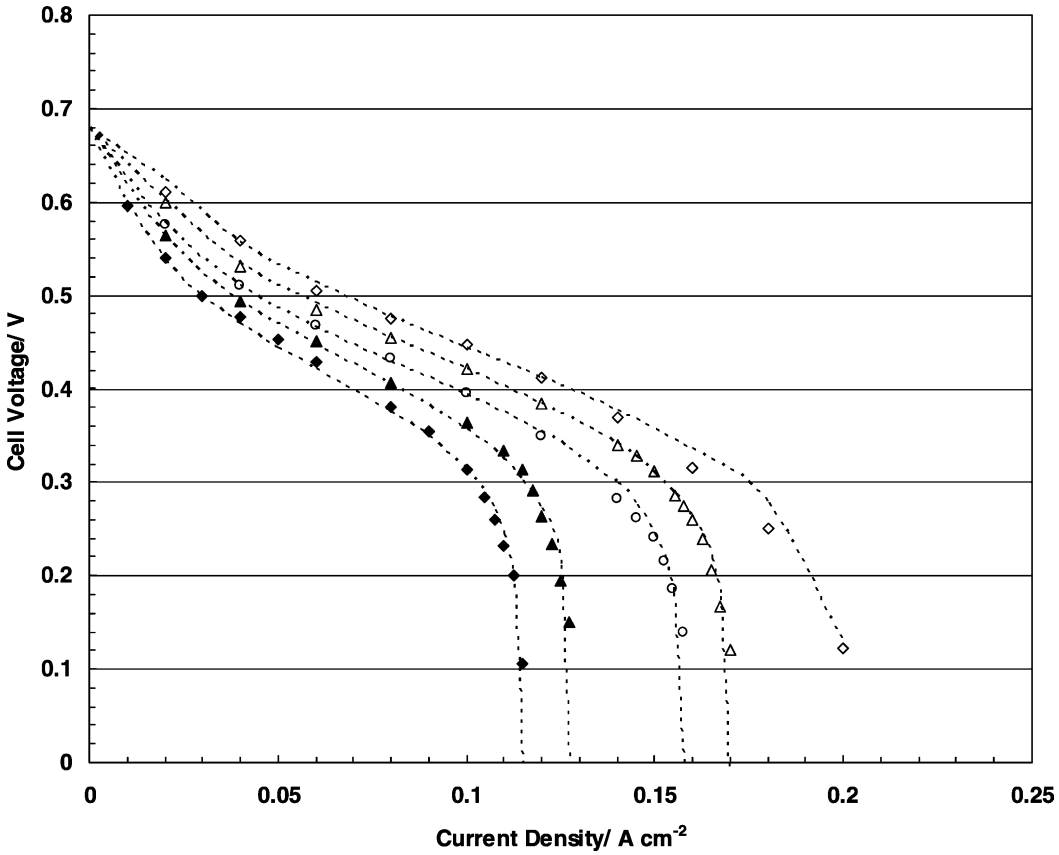

Fig. 6. Comparison between experimental data [11] and empirical equation based prediction for a cell operated with 0.75 M methanol solution supplied at a rate of 1.12 $cm^3\,min^{-1}$ with air fed cathodes pressurised at 2 bar (cell temperatures: (◆) 303.15; (▲) 313.151 K; (○) 323.15 K; (△) 333.15 K; (◇) 343.15 K).

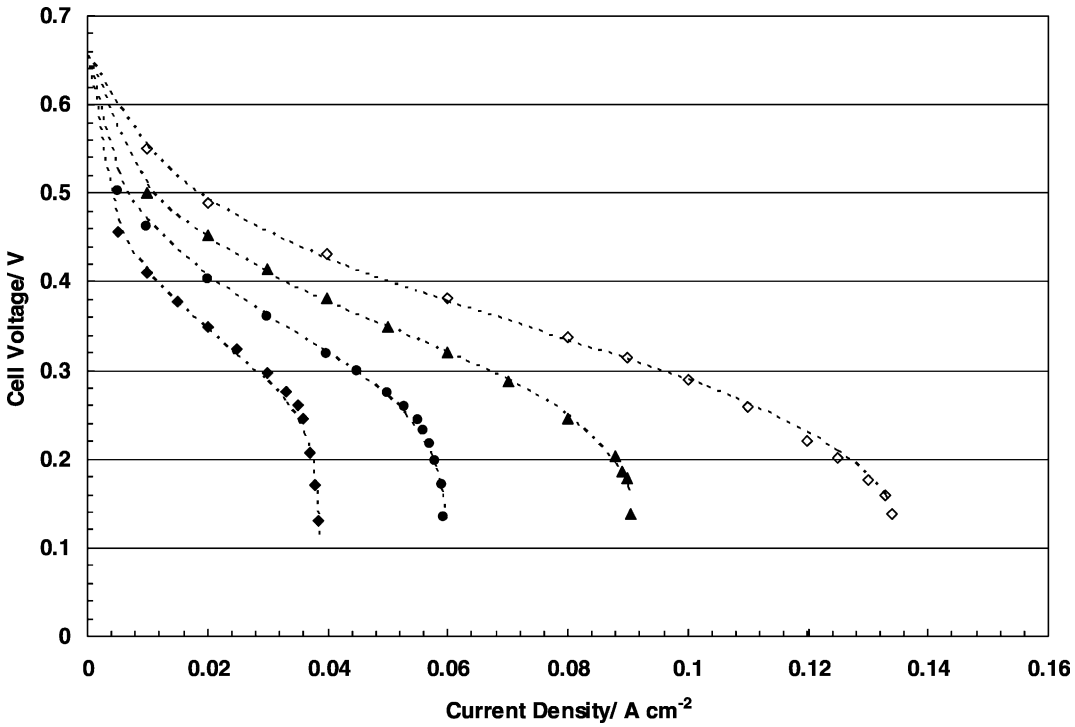

Fig. 7. The effect of varying parameter C_2 of Eq. (21) in the predicted cell response profiles. C_2 varies between 4.8 and 10.3 $cm^2\,A^{-1}$ ($E_o = 0.3$ V, $b = 0.12\,V\,dec^{-1}$, $R = 0.0001\,\Omega\,cm^2$, $C_1 = 0.059$ V).

A common weakness of many models for the DMFC is that they are only valid for narrow operating conditions. The current equation is applicable over a wide range of operating conditions. This is illustrated in Fig. 7 where we have used a set of coefficients representing one of our data sets and have varied parameter C_2 of Eq. (21) with all other parameters remaining constant. This data shows the ability of the present equation to predict the cell potential, current density profiles. In principle, this means that it can be used for a wide range of membrane electrode assembly materials and cell configurations that affect mass transfer; for example using different backing layers, carbon powders, etc. [8]. Alternatively, this data of Fig. 7 demonstrates the effect of varying the methanol concentration, leaving all other operating parameters constant [8,9].

Fig. 8 demonstrates the effect of decreasing the cell resistance in Eq. (21), which would be achieved by changing the membrane thickness or using alternative membrane

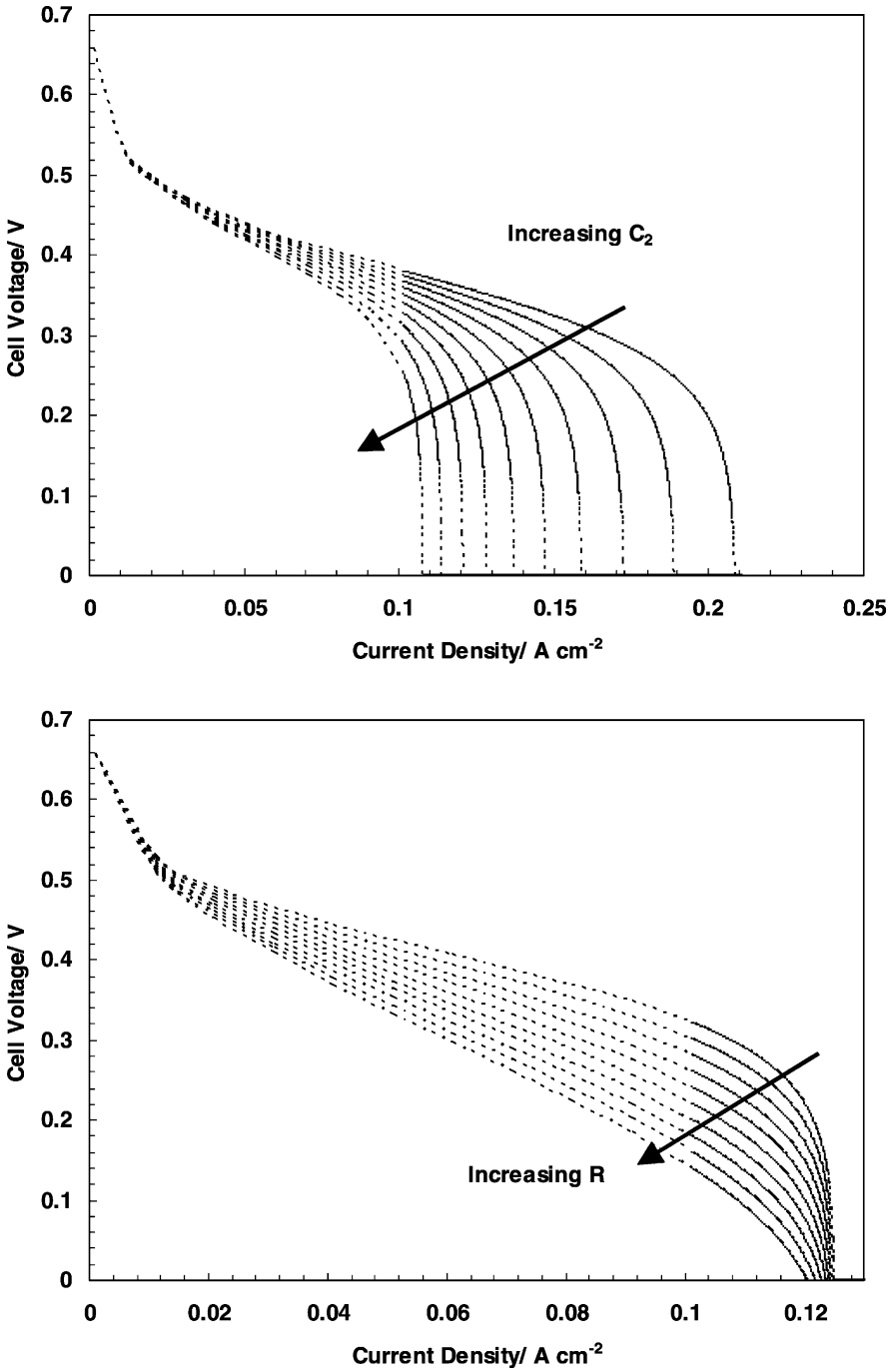

Fig. 8. The effect of decreasing cell resistance parameter R_e on cell voltage R varies from 0.0001 to 2.2001 $\Omega\,cm^2$ ($E_o = 0.3$ V, $b = 0.12\,V\,dec^{-1}$, $C_1 = 0.059$ V, $C_2 = 8\,cm^2\,A^{-1}$).

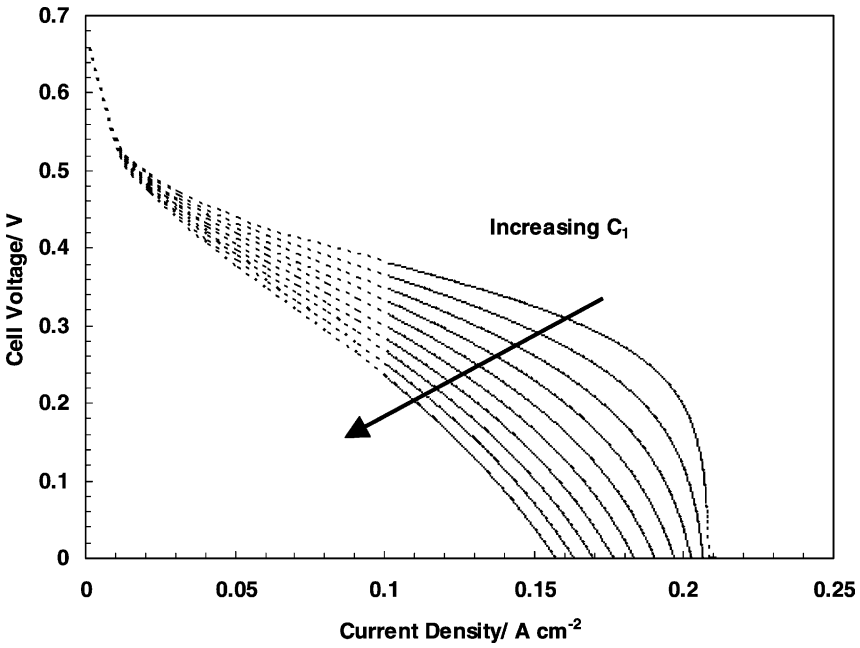

Fig. 9. The effect of varying parameter C_1 of Eq. (21) in the predicted cell response profiles.

materials [10]. As expected, as resistance increases, the mass transfer limitations remain essentially unaffected, but the voltage declines more rapidly.

Fig. 9 demonstrates the effect of decreasing parameter C_1, with all other parameters remaining constant. This situation represents, in general, limitations related to reaction kinetics which are attributable to a variety of reasons, e.g. decrease in cell temperature or poorer catalyst performance.

C_2 varies from 0.059 to 0.334 $cm^2\ A^-$ ($E_o = 0.3\,V$, $b = 0.12\,V\,dec^{-1}$, $R = 0.0001\,\Omega\,cm^2$ $C_1 = 0.059\,V$, $C_2 = 8\,cm^2\ A^{-1}$).

6. Conclusions

A semi-empirical equation, based on Tafel type kinetics and measured mass transport coefficients, has been developed to predict the voltage response of liquid fed direct methanol fuel cells over a wide range of operating conditions. The proposed equation is valid even in the case of very low current densities caused by, for example, the use of dilute methanol solutions or low cell temperatures. A further paper uses the model to determine appropriate kinetic and resistance parameters for the DMFC using data from two MEA structures.

Acknowledgements

The authors would like to acknowledge the following for support of this research: The European Commission for a TMR Marie Curie B20 and an IHP Marie Curie B30 research training grant to Dr. P. Argyropoulos. EPSRC and the MOD (through the joint grant scheme) supported Professor A.K. Shukla with a visiting fellowship. EPSRC supported C. Jackson through a Ph.D. studentship. The work was performed in research facilities provided through an EPSRC/HEFCE Joint Infrastructure Fund award no. JIF4NESCEQ.

References

[1] K. Kordesch, G. Simader, Fuel Cells and Their Applications, VCH Verlagsgesellschaft mbH, Weinheim, 1996.
[2] S. Srinivasan, E.A. Ticianelli, C.R. Derouin, A. Redondo, J. Power Sources 22 (1988) 359–375.
[3] J. Kim, S. Lee, S. Srinivansan, C.E. Chamberlin, J. Electrochem. Soc. 142 (8) (1995) 2670–2674.
[4] J.H. Lee, T.R. Lalk, J. Power Sources 73 (1998) 229–241.
[5] J.H. Lee, T.R. Lalk, A.J. Appleby, J. Power Sources 70 (1998) 258–268.
[6] J.H. Lee, T.R. Lalk, A modelling technique for fuel cell stack systems, ASME Dynamics Systems and Control Division, 1996.
[7] G. Squadrito, G. Maggio, E. Passalacqua, F. Lufrano, A. Patti, J. Appl. Electrochem. 29 (1999) 1449–1455.
[8] P. Argyropoulos, A. Shukla, K. Scott, C. Jackson, Fuel cells from fundamentals to systems. In press.
[9] K. Scott, W.M. Taama, P. Argyropoulos, J. Appl. Electrochem. 28 (12) (1999) 1389–1397.
[10] K. Scott, W.M. Taama, P. Argyropoulos, J. Membr. Sci. 171 (2000) 119–130.
[11] K. Scott, W.M. Taama, K. Sundmacher, J. Electroanal. Chem. 477 (1999) 97.
[12] A. Shukla, K. Scott, C. Jackson, Electrochim. Acta 111 (2002) 43.